Published in final edited form as:
Biochim Biophys Acta. 2006 June ; 1758(6): 781–788.

Ala-504 is a Determinant of Substrate Binding Affinity in the Mouse Na+/Dicarboxylate Cotransporter

Naomi Oshiro and **Ana M. Pajor***
Department of Biochemistry and Molecular Biology, University of Texas Medical Branch, Galveston, Texas 77555-0645

Abstract

The Na^+/dicarboxylate cotransporters from mouse (mNaDC1) and rabbit (rbNaDC1) differ in their ability to handle adipate, a six-carbon terminal dicarboxylic acid. The mNaDC1 and rbNaDC1 amino acid sequences are 75% identical. The rbNaDC1 does not transport adipate and only succinate produced inward currents under two-electrode voltage clamp. In contrast, oocytes expressing mNaDC1 had adipate-dependent inward currents that were about 60% of those induced by succinate. In order to identify domains involved in adipate transport, we examined the functional properties of a series of chimeric transporters made between mouse and rabbit NaDC1. We find that multiple transmembrane helices (TM), particularly TM 8, 9, and 10, are involved in adipate transport. In TM 10 there is only one amino acid difference between the two proteins, corresponding to Ala-504 in mouse and Ser-512 in rabbit NaDC1. The mNaDC1-A504S mutant had decreased adipate-dependent currents relative to succinate-dependent currents and an increase in the $K_{0.5}$ for both succinate and glutarate. We conclude that multiple amino acids from TM 8, 9 and 10 contribute to the transport of adipate in NaDC1. Furthermore, Ala-504 in TM 10 is an important determinant of $K_{0.5}$ for both adipate and succinate.

Keywords

adipate; succinate; NaDC1; sodium; *Xenopus* oocytes; substrate specificity

1. Introduction

Transport of citric acid cycle intermediates such as succinate and citrate across the plasma membrane is mediated by the Na^+/dicarboxylate cotransporters (NaDCs) belonging to the SLC13 gene family [1]. The low affinity transporter, NaDC1, is localized to the brush border membranes of renal proximal tubules and gastrointestinal tract. In contrast, the high affinity transporter, NaDC3, is expressed on the basolateral membrane of renal proximal tubule, as well as liver, placenta and brain. The physiological roles of NaDC1 involve absorption of dietary dicarboxylates in the intestine and reabsorption of filtered dicarboxylates in the kidney. NaDC3 and NaDC1 participate in organic anion secretion by contributing dicarboxylates to the organic anion exchangers [2]. NaDC1 in the kidney may affect the development of kidney stones through its regulation of urinary citrate concentrations [3]. Moreover, studies in flies and worms show a potential involvement of NaDCs in longevity since mutations in the genes encoding dicarboxylate transporter homologs in these organisms increased their lifespan [4, 5].

Although the NaDC1 and NaDC3 transporters have overlapping substrate specificity, there are some notable differences between them. In general, the NaDC1 transporters prefer four-carbon

*Corresponding author. Tel: 409-772-3434, Fax: 409-772-5102, Email: ampajor@utmb.edu.

dicarboxylates, such as succinate [6], whereas the NaDC3 transporters carry not only succinate but also longer and bulkier dicarboxylates such as glutarate and 2,3-dimethylsuccinate [7-9]. Interestingly, there are some species differences among the NaDC1 transporters, with the mouse NaDC1 having a substrate specificity similar to that of the NaDC3′s [10]. Recently, we constructed chimeras between the mouse and rabbit NaDC1 to show that putative transmembrane helices (TM) 3, 4, 7, and 8 are involved in glutarate transport in mNaDC1, with TM 3-4 making the greatest contribution to glutarate-dependent currents [11]. We also found that Gly-161 next to TM 4 affects the $K_{0.5}$ for glutarate but not for succinate [11].

Our preliminary experiments showed that the mouse and rabbit NaDC1 orthologs also differ in their ability to handle adipate, a six-carbon terminal dicarboxylate. The rabbit does not transport adipate, whereas the mouse transports adipate quite well. Therefore, the purpose of the present study was to identify domains and amino acids that determine adipate transport. Similar to our previous study, we found that multiple TMs are involved in producing adipate-induced inward currents. However, the main determinants of adipate transport are found in the C-terminal half of the protein, particularly TM 10 with contributions from TM 8 and 9, very different from the domains involved in glutarate transport [11]. Within TM 10, Ala-504 appears to be a determinant of adipate transport. Mutation from the mouse to the rabbit sequence at this position, mNaDC1-A504S, results in increases in the $K_{0.5}$ for both adipate and succinate, suggesting that Ala-504 is important for substrate binding in NaDC1.

2. Methods

2.1. Chimeric NaDC1 transporters

The NaDC1 chimeras consisting of mouse (m) NaDC1 (GenBank™ AF201903) and rabbit (rb) NaDC1 (GenBank™ U12186) are named using the number of transmembrane helices (TM) from mNaDC1 at the N-terminus and the letters M and R representing mouse and rabbit NaDC1, respectively. The current 11-TM secondary structure model of NaDC1 is based hydropathy analysis [12] and the location of N-glycosylation sites and epitopes [13,14]. The chimeras in this study were the same as those in our previous study, constructed using endogenous or introduced restriction sites followed by subcloning [11].

2.2. Site-directed mutagenesis

Mutagenesis in transmembrane helix (TM) 10 was carried out using the QuikChange™ site-directed mutagenesis kit (Stratagene) according to the manufacturer's directions. Briefly, the heat-denatured parental NaDC1 cDNA was annealed with both sense and anti-sense primers containing a desired mutation. After extension by polymerase chain reaction, the plasmid incorporating the mutagenic NaDC1 was transformed into the XL-1 blue strain of *E. coli.* The final mutants were verified by sequencing at the Protein Chemistry Laboratory of the University of Texas Medical Branch.

2.3. Preparation of Xenopus oocytes and injection of cRNA

Female *Xenopus laevis* were purchased from Xenopus I (Dexter, MI). Stage V and VI oocytes were dissected and incubated with collagenase as described previously [11]. The cRNA was made by *in vitro* transcription with the T7 mMessage mMachine kit (Ambion) using a linearized plasmid template containing cDNA of wild-type, chimeric, or mutant NaDC1. The cRNA was stored at -80°C until use. The oocytes were injected with 46-50 nl of cRNA the day after defolliculation and cultured at 18°C in Barth's medium supplemented with 5% heat-inactivated horse serum, 2.5 mM pyruvate, 100:μg/ml gentamycin sulfate, and either 50:μg/ml tetracycline or a mixture of 5:μg/ml ceftazidime (GlaxoSmithKline) and 100 U/ml penicillin-100:μg/ml streptomycin (Gibco). Experiments were performed three to six days after injections, and culture vials and medium were changed daily.

2.4. Electrophysiology

Substrate-induced inward currents mediated by wild-type, chimeric, or mutant NaDC1 transporters were measured using the two-electrode voltage clamp (TEVC) method as described previously [11]. The electrode resistance was less than 0.5 MS. Test voltage pulses of 100 msec between +50 and -150 mV in decrements of 20 mV were controlled using the pClamp6 program (Axon Instruments, Inc.). The holding membrane potential was set at -50 mV between the test pulses. The average of three measurements was recorded for the individual test pulses. For the experiments, the pulse protocol was applied first to oocytes equilibrated in choline buffer, then after addition of sodium buffer. The test solutions containing substrates in sodium buffer were then perfused over the oocytes. After measuring the substrate-induced currents, choline buffer was used to wash away the substrates, and subsequent experiments were performed followingrecovery of the initial currents in choline buffer. Experiments were repeated with oocytes from at least 3 different frogs.

The difference between steady-state currents with and without substrate in sodium buffer was defined as the substrate-dependent currents. The kinetic parameters were analyzed using SigmaPlot software (Jandel Scientific), and the steady-state substrate-evoked currents were fitted to the Michaelis-Menten equation: $I = I_{max} * [S] / (K_{0.5} + [S])$, where I is the current, I_{max} is the maximum current at saturating substrate concentration, [S] is the substrate concentration, and $K_{0.5}$ is the substrate concentration producing half of the maximum currents. Statistical analysis was done using the SigmaStat program (Jandel Scientific).

3. RESULTS

3.1. Voltage-dependent currents in wild-type NaDC1 transporters

In our previous studies, we found that mNaDC1 and rbNaDC1 have functional differences in glutarate transport, although glutarate is only one carbon longer than succinate [6,10,11,15]. Therefore, in this study we tested whether these transporters also differ in their handling of adipate, a six-carbon terminal dicarboxylic acid. As shown in Fig. 1, mNaDC1 had large substrate-dependent inward currents induced by both adipate and succinate whereas rbNaDC1 had inward currents with only succinate. Adipate and succinate-dependent currents were not detected in control oocytes (data not shown and [16]).

3.2. Kinetics of adipate-induced currents in mNaDC1

The concentration dependence of steady-state adipate-induced currents was examined in oocytes expressing mNaDC1. The results of a single experiment at -50 mV are shown in Fig. 2A and the means of three experiments at different voltages are in Figs 2B, C. The $K_{0.5}$ for adipate was 0.54 mM, and the I_{max} was -348 nA (Fig. 2A). In three experiments, the mean $K^{adipate}_{0.5}$ was 0.70 ± 0.12 mM (mean ± SEM), and the $I^{adipate}_{max}$ was -239 ± 55 nA at -50 mV. The voltage dependence of $K^{adipate}_{0.5}$ and $I^{adipate}_{max}$ are shown in Figs. 2B, C. The $K^{adipate}_{0.5}$ was voltage insensitive at potentials more negative than -50 mV and gradually increased as the membrane potential became more positive. For example, at -150 mV, $K^{adipate}_{0.5}$ was 0.47 ± 0.06 mM, and at +50 mV, $K^{adipate}_{0.5}$ was 2.22 ± 0.37 mM (mean ± SEM, n = 3) (Fig. 2B). The maximum adipate-inducedinward currents, $I^{adipate}_{max}$, were sensitive to the membrane potential, with a 3.6-fold increase between +50 and -150 mV (Fig. 2C).

3.3. Substrate-induced currents in chimeric NaDC1 transporters

A series of chimeras, consisting of increasing substitutions by mNaDC1 at the N-terminus (Fig. 3) were used to examine adipate-dependent currents after expression in *Xenopus* oocytes. The substrate-induced currents were measured using the same pulse protocol as the one shown in

Fig. 1, but for simplicity only the data at -50 mV are shown (Fig. 4). The results were similar at all voltages (results not shown). All of the chimeras exhibited succinate-induced currents similar to those of the wild-type mouse or rabbit NaDC1, but differed in their adipate-induced currents (Fig. 4A). We also tested some chimeras containing rabbit NaDC1 at the N-terminus: 7RM (containing TM 1-7 of rbNaDC1 and TM 8-11 of mNaDC1) and 8RM (TM 1-8 of rbNaDC1 and TM 9-11 of mNaDC1). However, the succinate-induced currents were too small for further experiments, similar to our previous observations[11,17].

At -50 mV, the adipate-dependent currents in mNaDC1 were 61% of the succinate-induced currents, whereas in rbNaDC1 there were no detectable currents in the presence of adipate (Figs. 4A, B). The chimeras showed increases in adipate-dependent currents relative to the succinate-induced currents, depending on the number of TM from mNaDC1 at the amino terminus. There were statistically significant differences between rbNaDC1 and the 6MR chimera, the 7MR and 8MR chimeras, the 8MR and 9MR chimeras, and the 9MR and 10MR chimeras (Fig. 4B). Overall, the most important contributions to adipate-dependent currents were made by TM 10 with some contributions from TM 8 and 9. TM 7 and 11 do not appear to be involved in adipate transport since there were no differences between the 6MR and 7MRchimeras or between the 10 MR chimera and wild-type mNaDC1 (Fig. 4B). Our previous study with glutarate examined both substrate-dependent currents and the transport specificity ratio (TSR), a protein expression-independent constant calculated with values from dual-label competitive uptakes, to investigate changes in relative substrate specificity in the transition state [11]. However, it was not possible to measure the TSR for adipate and succinate in this study due to high background uptake of ^{14}C-adipate in control oocytes, resulting in inaccurate TSR values (data not shown).

3.4. Mutagenesis in TM 10

The largest contribution to adipate-induced currents appears to be from TM 10, containing amino acids 519-586 (mNaDC1 numbering). There is only one amino acid difference between mouse and rabbit NaDC1 in TM10. The mNaDC1 has an alanine at position 504 whereas rbNaDC1 has a serine at the equivalent position 512. The A504S mutant of mNaDC1 was expressed in *Xenopus* oocytes in paired experiments with the wild-type mNaDC1, and substrate-dependent currents were measured in the presence of adipate and succinate (Fig. 5A). As shown in Fig. 5B, the adipate-dependent currents relative to the succinate-dependent currents were 40.4 ± 3.9% in the A504S mutant, significantly lower than the adipate currents relative to succinate in mNaDC1 of 59.3 ± 0.8% (n = 3 paired experiments). Since TM 11 does not seem to participate in adipate transport, the A504S mutant of mNaDC1 should correspond to the 9MR chimera, which contains rabbit sequence from TM 10 and 11 (Fig. 3). In fact, there were no significant differences in adipate:succinate currents between the A504S mutant and the 9MR chimera (Fig. 4B). The S512A mutant of rbNaDC1 was also tested but the mutation of only one residue is not enough to add function to rbNaDC1, compared with removing one of at least three residues in theA504S mutant of mNaDC1. The currents in the rbNaDC1-S512A mutant were the same as in wild-type rbNaDC1 (not shown).

The kinetics of the A504S mutant of mNaDC1 were examined with both adipate and succinate. This single mutation at position 504 resulted in increases in the $K_{0.5}$ for both adipate and succinate compared with the parental transporter, mNaDC1 (Fig. 6, 7). In the single experiment shown in Fig. 6A, the $K^{adipate}_{0.5}$ for the A504S mutant was 1.25 mM and $I^{adipate}_{max}$ was -797 nA at -50 mV. In three experiments, the mean $K^{adipate}_{0.5}$ was 1.25 ± 0.04 mM (mean ± SEM, n = 3), significantly different from the mean $K^{adipate}_{0.5}$ of 0.7 mM in mNaDC1 (Fig. 2). The voltage dependence of $K^{adipate}_{0.5}$ and $I^{adipate}_{max}$ are shown in Figs. 6B, C (n=3 experiments). The $K^{adipate}_{0.5}$ gradually increased from 0.84 mM at -150 mV to 4.61 mM at +50 mV (Fig.

6B). The $I^{adipate}_{max}$ was also voltage sensitive with almost a 5-fold increase in adipate-induced currents between +50 mV (-364 nA) and -150 mV (-1743 nA) (Fig. 6C).

Interestingly, the affinity for succinate in the mNaDC1-A504S mutant also changed. The A504S mutant had a $K^{succinate}_{0.5}$ of 291 μM and $I^{succinate}_{max}$ of -1319 nA at -50 mV in the single experiment shown in Fig. 7A. The mean $K^{succinate}_{0.5}$ for this mutant was 270 ± 32 μM (mean ± SEM, n = 3), significantly different from the $K^{succinate}_{0.5}$ of 99 ± 15 μM for the parental mNaDC1 but similar to the previously reported rbNaDC1 value of 203 ± 30 μM[6,11]. The voltage dependence of $K^{succinate}_{0.5}$ was altered in the A504S mutant compared with the parental mNaDC1 (Fig. 7B for A504S, Fig. 2B for mNaDC1). The $K^{succinate}_{0.5}$ was relatively insenstive to voltage between -50 and +50 mV, but increased at more negative voltages (427 μM at -150 mV and 257 μM at +50 mV). The $I^{succinate}_{max}$ was sensitive to membrane potential with an increase of about 6- fold between +50 (-331 nA) and -150 mV (-2118 nA) (Fig. 7C).

One possible explanation for the change in $K^{succinate}_{0.5}$ in the mNaDC1-A504S mutant is that the affinity for sodium has decreased, and the 100 mM Na^+ concentration used for the assay is no longer saturating. This was tested by examining the sodium activation of succinate-induced currents in the mNaDC1-A504S mutant. In a single experiment, the half saturation constant, $K^{sodium}_{0.5}$, was 11 mM at -50 mV (data not shown), lower than the previously reported value of 23 mM for wild-type mNaDC1 [10]. The Hill coefficient was 2.24 in the mutant (not shown) compared with 2.1 in the wild-type [10]. Therefore, the increased $K^{succinate}_{0.5}$ in the mNaDC1-A504S mutant compared with the parental mNaDC1 transporter is not due to a decrease in sodium affinity.

4. Discussion

The mouse and rabbit NaDC1 transporters differ in their ability to transport adipate, a six-carbon dicarboxylate. The mNaDC1 exhibits large adipate-induced inward currents whereas rbNaDC1 has no measurable currents in the presence of adipate. To identify protein domains involved in determining differences in adipate transport, a series of chimeras was constructed between mNaDC1 and rbNaDC1, and substrate-dependent currents were measured using two-electrode voltage clamp. We found that multiple transmembrane helices (TM) including TM 8, 9, and 10 are involved in adipate transport. Furthermore, the mNaDC1-A504S mutant exhibited changes in $K_{0.5}$ for both adipate and succinate, suggesting that Ala-504 in TM 10 is involved in recognition of both adipate and succinate in NaDC1.

The domains in NaDC1 involved in adipate transport are also involved in transport of other substrates. For example, the differences in the affinity for citrate between the human and rabbit NaDC1 are determined by residues in TM 7, 10, and 11 [17]. Asp-373 in TM 8 is important in both substrate and cation binding, and exhibits differences in accessibility depending on conformational state [18]. TM 9 and 10 appear to form part of the substrate translocation pathway in NaDC1 [19,20]. Interestingly, different TM are involved in handling glutarate and adipate in NaDC1. TM 3-4 are the most important in determining differences between mNaDC1 and rbNaDC1 in the transport of glutarate, with some contributions also from TM 7 and 8 [11]. It is likely that succinate, adipate and glutarate have some common interactions with amino acids in NaDC1, and there are additional interactions that are specific to adipate and glutarate.

Although there is no information at this time on the substrate binding pocket in NaDC1, it may have some features in common with substrate binding pockets of other broad-specificity transporters, such as the peptide transporter, PepT1 [21]. PepT1 can interact with many differentclasses of compounds that conform to a given substrate template structure, which contains at least four contact sites between the substrate and transport protein [21]. Substrates that can adopt the appropriate conformation interact with high affinity with the PepT1 protein.

Similar to the PepT1 substrates, the dicarboxylates transported by NaDC1 are flexible molecules that can adopt multiple stable conformations [22,23]. The differences in the substrate binding pockets between the rabbit and mouse NaDC1 are probably the result of differences in substrate:protein contact points or differences in the size of the substrate binding pocket. For example, mNaDC1 may have a larger substrate binding pocket to accomodate longer chain dicarboxylates.

The mutation of alanine 504 in mNaDC1 to the serine found at the equivalent position in rbNaDC1 produced increases in the $K_{0.5}$ for both adipate and succinate. The wild-type rbNaDC1 exhibits very high discrimination between the two substrates since there were no currents induced by adipate. Although the decrease in adipate affinity in mNaDC1-A504S is approaching the rabbit phenotype, the discrimination between substrates has not increased, since the $K_{0.5}$ increased for both succinate and adipate. This result suggests that Ala-504 may be an important determinant of dicarboxylate binding but not of distinguishing between substrates. Possibly the interaction between Ala-504 and residues in TM 8 and 9 is required for discrimination between substrates. In contrast to the functional changes in the mNaDC1-A504S mutant, we observed no changes in the rbNaDC1-S512A mutant. In our previous study, the rbNaDC1-S512C mutant was not expressed on the plasma membrane, suggesting that a cysteine at this position produces a misfolded protein [20]. In the present study, the rbNaDC1-S512A mutant had similar substrate-dependent inward currents as the wild-type rbNaDC1 (not shown). Since multiple amino acids are likely to be required for the transport of adipate, changing a single residue in rbNaDC1 may not be enough to add function. In the mNaDC1, changing a single residue in the A504S mutant still leaves other residues in TM 8 and 9, with the result of reducing substrate affinity but notcompletely abolishing transport of adipate. However, we cannot completely rule out the possibility that the changes in $K_{0.5}$ for substrates in the mNaDC1-A504S mutant are due to indirect effects on the substrate binding site as a result of changes in overall protein structure or in the number of water molecules in the substrate binding pocket.

At present, the reason for the functional difference between alanine and serine in binding adipate in NaDC1 has not been determined. The size of alanine and serine residues are not very different, 26.3 and 30.4 $Å^3$, respectively, and serine is thought of as a hydroxylated version of alanine [24]. However, the hydroxyl group in serine renders it more hydrophilic than alanine. In addition, serine residues can introduce a bend angle into a transmembrane helix compared with alanine, which could potentially displace other residues [25]. Serines have been shown to participate in substrate and cation binding in transport proteins. In the Na^+/sulfate transporter, also a member of the SLC13 family, serines are found at positions 260 and 288, whereas alanines are found at the equivalent positions in the dicarboxylate transporters. Mutation of these serines to alanine decreases affinity for sulfate and alters cation specificity [26]. A similar involvement of serines in substrate and cation binding has been seen in the vesicular monoamine transporter, VMAT [27], the Na^+-Cl^--dependent serotonin transporter [28], and the Na^+/K^+-ATPase [29].

The voltage-dependence of adipate transport in the wild-type mNaDC1 is very similar to the voltage-dependence of succinate transport in other NaDC1 orthologs from rabbit, human [6, 30] and mouse (results not shown) and in high-affinity NaDC3 orthologs from human, mouse and flounder [9,31,32]. The maximal substrate-dependent inward current, I_{max}, increases with more negative voltages indicating that voltage-dependent steps are a general property of sodium-dependent transporters from the SLC13 family. This voltage dependence suggests that a rate-limiting step in the transport cycle involves translocation of negative charges through the electric field as the empty carrier reorients to face the outside of the cell [31,33]. The $K_{0.5}$ in thesetransporters is relatively insensitive to negative voltages, indicating that substrate binding is not affected by electric field, despite the fact that the substrates are divalent anions.

Many of these transporters also exhibit an increase in $K_{0.5}$ at positive voltages. The voltage-dependence of adipate transport in the mNaDC1-A504S mutant is very similar to that of the wild-type mNaDC1. In contrast, the voltage-dependence of succinate transport in the mutant is different from the parental transporter, with an increase in $K^{\text{succinate}}_{0.5}$ as the voltage becomes more negative. A similar effect of voltage on $K_{0.5}$ has been observed for citrate binding in wild-type rat NaDC1 [34], the Na^+/Cl^-/GABA transporter [35], and the H^+-coupled oligopeptide transporter [36]. At least one of the cation binding sites and the substrate binding site appear to be located close together in the C-terminal half of NaDC1 [37], so it is possible that the A504S mutation may affect the voltage-dependent binding of Na^+ ions, leading to a change in voltage-dependence in $K^{\text{succinate}}_{0.5}$. Nevertheless, it is not clear why substitution of one neutral amino acid by another in the mNaDC1-A504S mutant should result in an alteration in voltage dependence of succinate binding but not adipate.

In conclusion, the mouse and rabbit NaDC1 exhibit differences in the transport of the six-carbon dicarboxylate, adipate. The mNaDC1 has adipate-dependent inward currents whereas rbNaDC1 exhibits no currents in the presence of adipate. The results of the chimera and mutagenesis studies show that the differences in adipate transport between mNaDC1 and rbNaDC1 are determined predominantly by Ala-504 found in TM 10, with contributions from residues in TM 8 and 9. Interestingly, the amino terminal half of mNaDC1 does not play a major role in adipate recognition, unlike our previous findings with glutarate transport, although adipate and glutarate differ in length by only one carbon [11]. We conclude that TM 8, 9 and 10 are involved in adipate transport in NaDC1. Ala-504 in TM 10 is an important determinant ofdicarboxylate binding in the initial Michaelis complex, and other residues in TM 8 and 9 also participate in adipate recognition.

Acknowledgements

We thank Kathleen Randolph for her assistance in preparation of oocyte solutions. This study was supported by National Institutes of Health Grant DK46269.

References

1. Pajor AM. Molecular properties of the SLC13 family of dicarboxylate and sulfate transporters. Pflugers Arch 2006;451:597–605. [PubMed: 16211368]
2. Dantzler WH, Evans KK. Effect of αKG in lumen on PAH transport by isolated perfused proximal tubules. Am. J. Physiol 1996;271:F521–F526. [PubMed: 8853413]
3. Pak CYC. Etiology and treatment of urolithiasis. Am. J. Kidney Diseases 1991;18:624–637. [PubMed: 1962646]
4. Fei YJ, Inoue K, Ganapathy V. Structural and functional characteristics of two sodium-coupled dicarboxylate transporters (ceNaDC1 and ceNaDC2) from *Caenorhabditis elegans* and their relevance to life span. J. Biol. Chem 2003;278:6136–6144. [PubMed: 12480943]
5. Rogina B, Reenan RA, Nilsen SP, Helfand SL. Extended life-span conferred by cotransporter gene mutations in *Drosophila*. Science 2000;290:2137–2140. [PubMed: 11118146]
6. Pajor AM, Hirayama BA, Loo DDF. Sodium and lithium interactions with the Na^+/dicarboxylate cotransporter. J. Biol. Chem 1998;273:18923–18929. [PubMed: 9668069]
7. Burckhardt BC, Lorenz J, Kobbe C, Burckhardt G. Substrate specificity of the human renal sodium dicarboxylate cotransporter, hNaDC-3, under voltage-clamp conditions. Am. J. Physiol. Renal Physiol 2005;288:F792–F799. [PubMed: 15561973]
8. Chen X, Tsukaguchi H, Chen XZ, Berger UV, Hediger MA. Molecular and functional analysis of SDCT2, a novel rat sodium-dependent dicarboxylate transporter. J. Clin. Invest 1999;103:1159–1168. [PubMed: 10207168]
9. Pajor AM, Gangula R, Yao X. Cloning and functional characterization of a high-affinity Na^+/dicarboxylate cotransporter from mouse brain. Am. J. Physiol. Cell Physiol 2001;280:C1215–C1223. [PubMed: 11287335]

10. Pajor AM, Sun NN. Molecular cloning, chromosomal organization, and functional characterization of a sodium-dicarboxylate cotransporter from mouse kidney. Am. J. Physiol. Renal Physiol 2000;279:F482–F490. [PubMed: 10966927]
11. Oshiro N, King SC, Pajor AM. Transmembrane helices 3 and 4 are involved in substrate recognition by the Na^+/dicarboxylate cotransporter, NaDC1. Biochemistry 2006;45:2302–2310. [PubMed: 16475819]
12. Rao JKM, Argos P. A conformational preference parameter to predict helices in integral membrane proteins. Biochim. Biophys. Acta 1986;869:197–214. [PubMed: 2935194]
13. Pajor AM, Sun N. Characterization of the rabbit renal Na^+-dicarboxylate cotransporter using antifusion protein antibodies. Am. J. Physiol 1996;271:C1808–C1816. [PubMed: 8997180]
14. Zhang FF, Pajor AM. Topology of the Na^+/dicarboxylate cotransporter: the N-terminus and hydrophilic loop 4 are located intracellularly. Biochim. Biophys. Acta 2001;1511:80–89. [PubMed: 11248207]
15. Pajor AM, Sun N. Functional differences between rabbit and human Na^+-dicarboxylate cotransporters, NaDC-1 and hNaDC-1. Am. J. Physiol 1996;271:F1093–F1099. [PubMed: 8946005]
16. Oshiro N, Pajor AM. Functional characterization of high-affinity Na^+/dicarboxylate cotransporter found in *Xenopus laevis* kidney and heart. Am. J. Physiol. Cell Physiol 2005;289:C1159–C1168. [PubMed: 15944208]
17. Kahn ES, Pajor AM. Determinants of substrate and cation affinities in the Na^+/dicarboxylate cotransporter. Biochemistry 1999;38:6151–6156. [PubMed: 10320342]
18. Yao X, Pajor AM. Arginine-349 and aspartate-373 of the Na^+/dicarboxylate cotransporter are conformationally sensitive residues. Biochemistry 2002;41:1083–1090. [PubMed: 11790133]
19. Pajor AM. Conformationally sensitive residues in transmembrane domain 9 of the Na^+/dicarboxylate co-transporter. J. Biol. Chem 2001;276:29961–29968. [PubMed: 11399753]
20. Pajor AM, Randolph KM. Conformationally sensitive residues in extracellular loop 5 of the Na^+/dicarboxylate co-transporter. J. Biol. Chem 2005;280:18728–18735. [PubMed: 15774465]
21. Bailey PD, Boyd CA, Bronk JR, Collier ID, Meredith D, Morgan KM, Temple CS. How to Make Drugs Orally Active: A Substrate Template for Peptide Transporter PepT1. Angew. Chem. Int. Ed. Engl 2000;39:505–508. [PubMed: 10671239]
22. Nguyen TH, Hibbs DE, Howard ST. Conformations, energies, and intramolecular hydrogen bonds in dicarboxylic acids: implications for the design of synthetic dicarboxylic acid receptors. J. Comput. Chem 2005;26:1233–1241. [PubMed: 15962275]
23. Price DJ, Roberts JD, Jorgensen WL. Conformational complexity of succinic acid and its monoanion in the gas phase and in solution: *Ab initio* calculations and Monte Carlo simulations. J. Am. Chem. Soc 1998;120:9672–9679.
24. Cohen A, Ellis P, Kresge N, Soltis SM. MAD phasing with krypton. Acta Crystallogr. D. Biol. Crystallogr 2001;57:233–238. [PubMed: 11173469]
25. Ballesteros JA, Deupi X, Olivella M, Haaksma EE, Pardo L. Serine and threonine residues bend alpha-helices in the χ_1=g^- conformation. Biophys. J 2000;79:2754–2760. [PubMed: 11053148]
26. Li H, Pajor AM. Serines 260 and 288 are involved in sulfate transport by hNaSi-1. J. Biol. Chem 2003;278:37204–37212. [PubMed: 12857732]
27. Merickel A, Rosandich P, Peter D, Edwards RH. Identification of residues involved in substrate recognition by a vesicular monoamine transporter. J. Biol. Chem 1995;270:25798–25804. [PubMed: 7592763]
28. Sur C, Betz H, Schloss P. A single serine residue controls the cation dependence of substrate transport by the rat serotonin transporter. Proc. Natl. Acad. Sci. U. S. A 1997;94:7639–7644. [PubMed: 9207145]
29. Blostein R, Wilczynska A, Karlish SJ, Arguello JM, Lingrel JB. Evidence that Ser^{775} in the alpha subunit of the Na,K-ATPase is a residue in the cation binding pocket. J. Biol. Chem 1997;272:24987–24993. [PubMed: 9312104]
30. Yao X, Pajor AM. The transport properties of the human renal Na^+/dicarboxylate cotransporter under voltage clamp conditions. Am. J. Physiol 2000;279:F54–F64.

31. Burckhardt BC, Steffgen J, Langheit D, Muller GA, Burckhardt G. Potential-dependent steady-state kinetics of a dicarboxylate transporter cloned from winter flounder kidney. Pflugers Arch 2000;441:323–330. [PubMed: 11211120]

32. Wang H, Fei YJ, Kekuda R, Yang-Feng TL, Devoe LD, Leibach FH, Prasad PD, Ganapathy V. Structure, function, and genomic organization of human Na^+-dependent high-affinity dicarboxylate transporter. Am. J. Physiol. Cell Physiol 2000;278:C1019–C1030. [PubMed: 10794676]

33. Geck P, Heinz E. Coupling in secondary transport. Effect of electrical potentials on the kinetics of ion linked co-transport. Biochim. Biophys. Acta 1976;443:49–53. [PubMed: 8129]

34. Chen XZ, Shayakul C, Berger UV, Tian W, Hediger MA. Characterization of rat Na^+-dicarboxylate cotransporter. J. Biol. Chem 1998;273:20972–20981. [PubMed: 9694847]

35. Mager S, Naeve J, Quick M, Labarca C, Davidson N, Lester HA. Steady states, charge movements, and rates for a cloned GABA transporter expressed in *Xenopus* oocytes. Neuron 1993;10:177–188. [PubMed: 7679914]

36. Mackenzie B, Loo DD, Fei Y, Liu WJ, Ganapathy V, Leibach FH, Wright EM. Mechanisms of the human intestinal H^+-coupled oligopeptide transporter hPEPT1. J. Biol. Chem 1996;271:5430–5437. [PubMed: 8621398]

37. Griffith DA, Pajor AM. Acidic residues involved in cation and substrate interactions in the Na^+/dicarboxylate cotransporter, NaDC-1. Biochemistry 1999;38:7524–7531. [PubMed: 10360950]

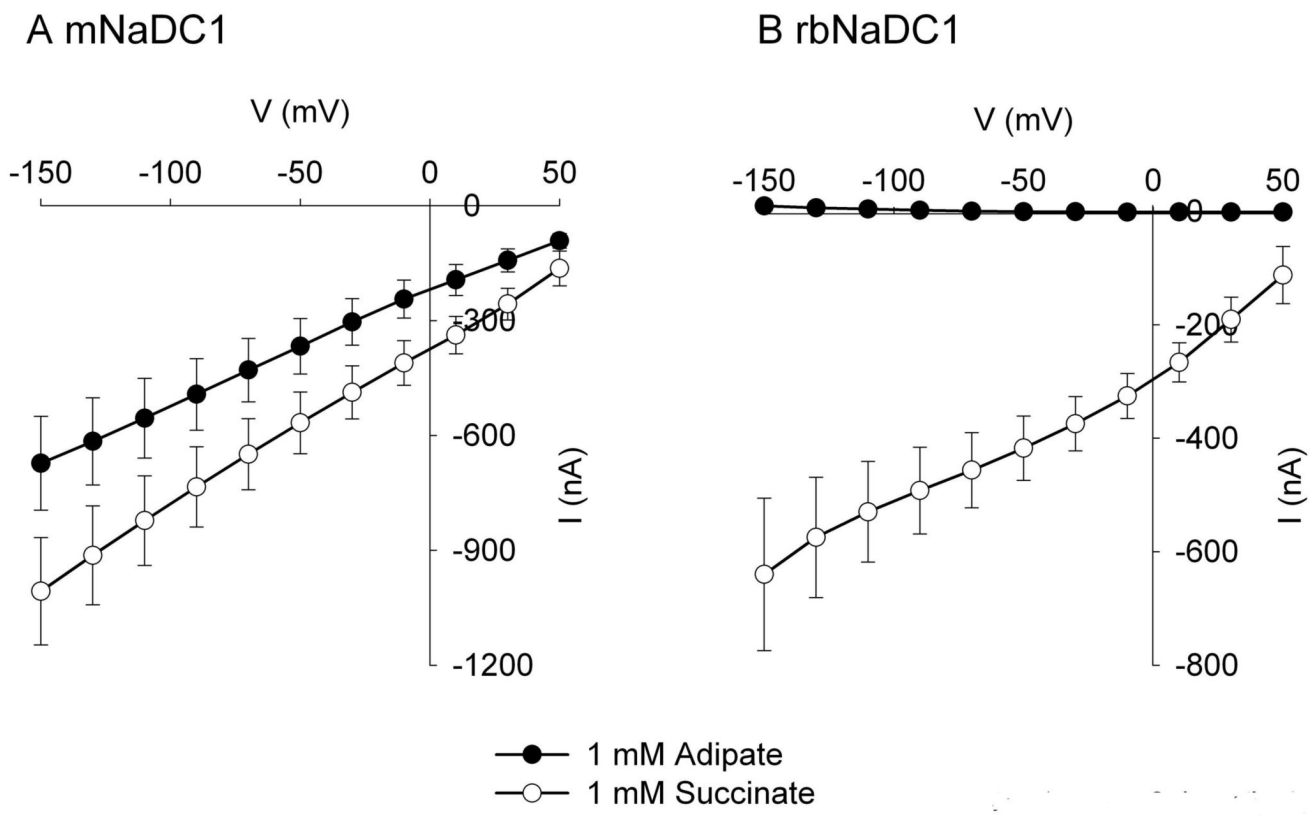

Fig. 1.

The voltage dependence of steady-state substrate-dependent currents in mNaDC1 and rbNaDC1 expressed in *Xenopus* oocytes. Adipate- and succinate-induced currents in mNaDC1 (A) and rbNaDC1 (B) are shown as a function of different voltages. The concentration of the substrates was 1 mM. The mNaDC1-mediated inward currents were seen in the presence of both adipate and succinate at all tested voltages. In contrast, rbNaDC1-mediated inward currents were only detected in the presence of succinate. The data shown are mean ± SEM, n = 14 frogs.

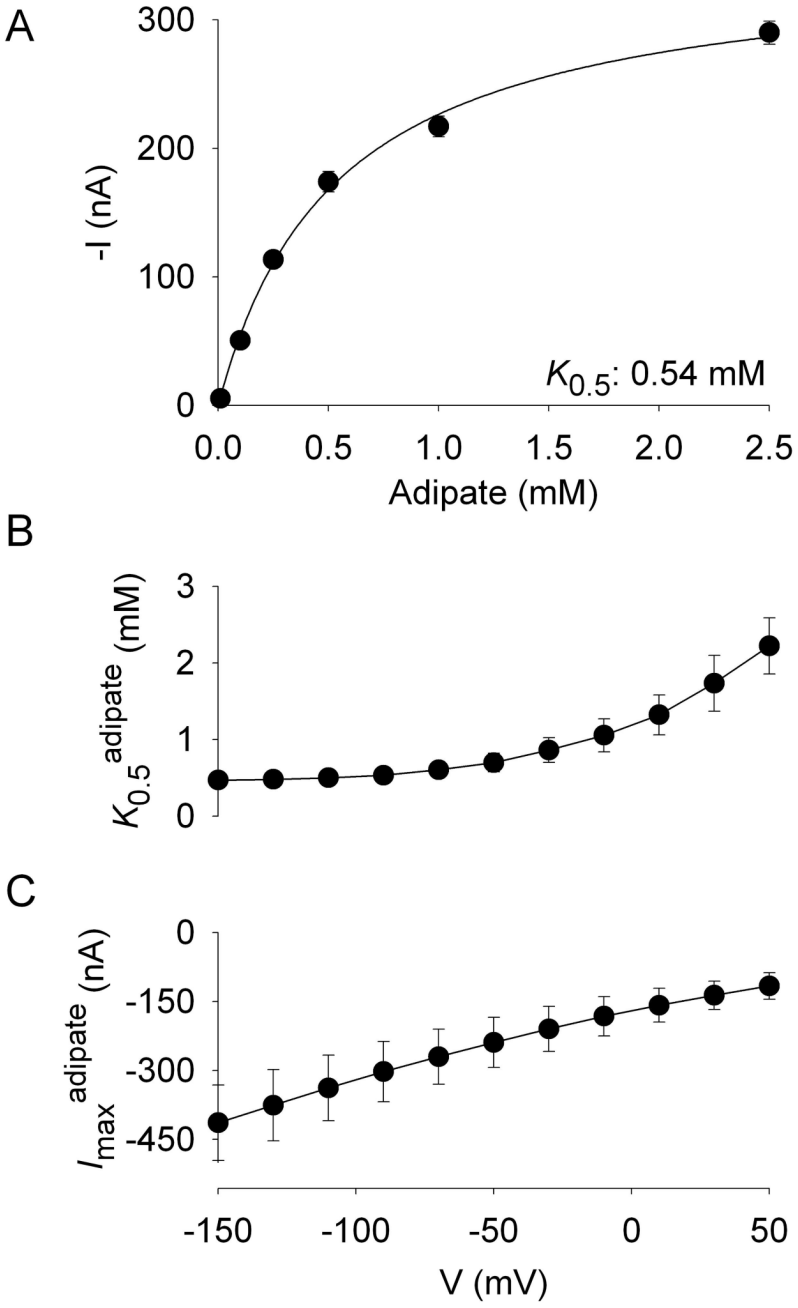

Fig. 2.

Kinetics of adipate-induced currents mediated by mNaDC1. (A) The concentration dependence of steady-state adipate-induced currents at -50 mV in oocytes expressing mNaDC1. The result from a single experiment is shown in this panel, and each data point represents the mean ± range of duplicate measurements in a single oocyte. The adipate concentrations were between 0.01 mM and 2.5 mM. The $K_{0.5}$ for adipate is 0.54 mM and I_{max} is -348 nA. (B) and (C), The voltage dependence of the mean $K_{0.5}$ and I_{max} for adipate, respectively. The data shown are mean ± SEM, n = 3 frogs.

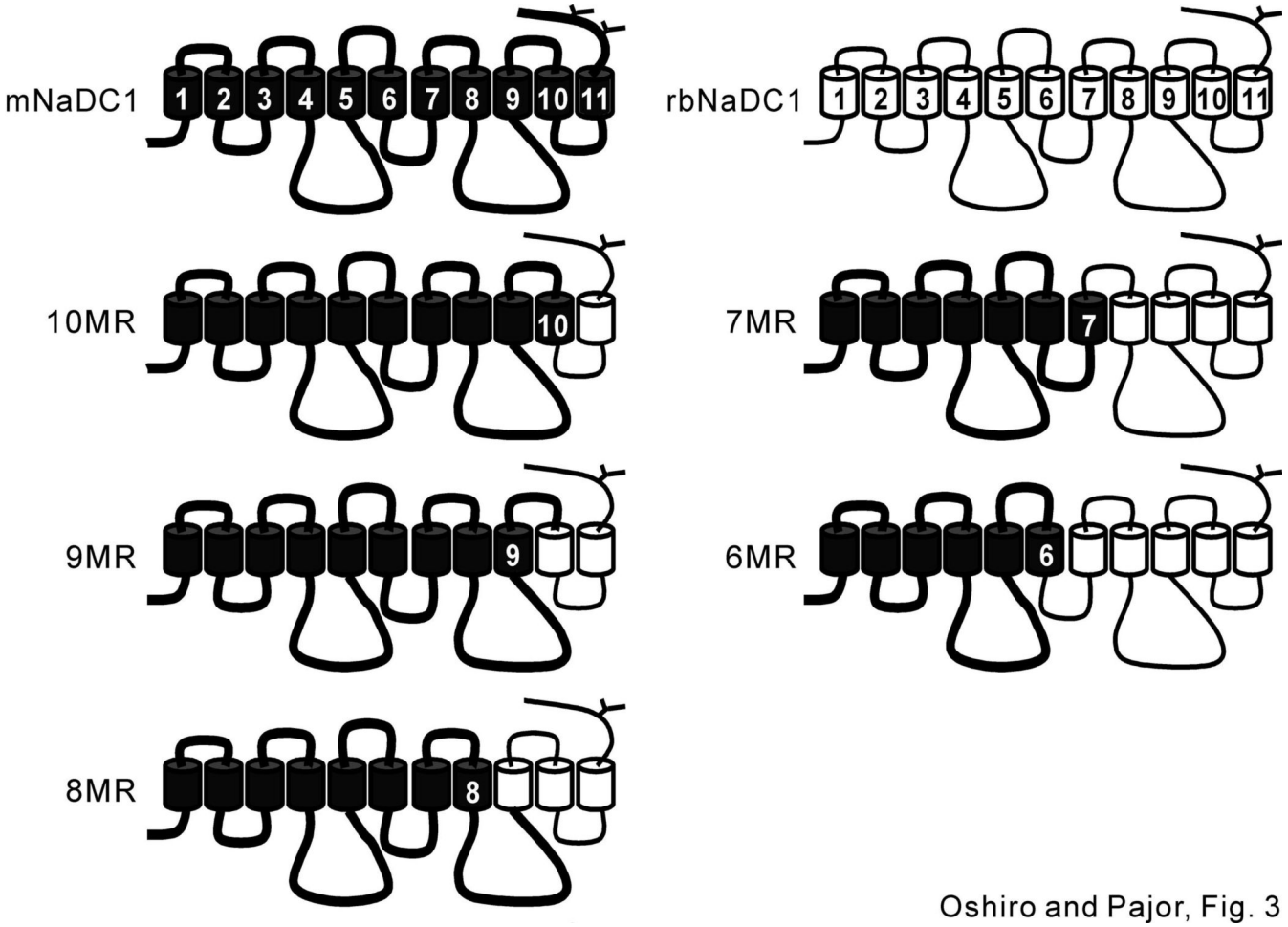

Fig. 3.

Secondary structure models of the mNaDC1-rbNaDC1 chimeras. These chimeras were used in a previous study to examine glutarate transport {Oshiro, King, et al. 2006 755/id}. The chimeras are named using the number of TM from mNaDC1 at the N-terminus and the letters M (mouse) and R (rabbit). The junctions between chimeras are at positions: 284 (6MR), 341 (7MR), 427 (8MR), 489 (9MR) and 518 (10MR). The transmembrane helices (TM) and connected loops from mNaDC1 are shown as filled cylinders and bold lines, and those from rbNaDC1 in open cylinders and fine lines. The *N*-glycosylation site is indicated by the Y. The extracellular side is at the top of the figure.

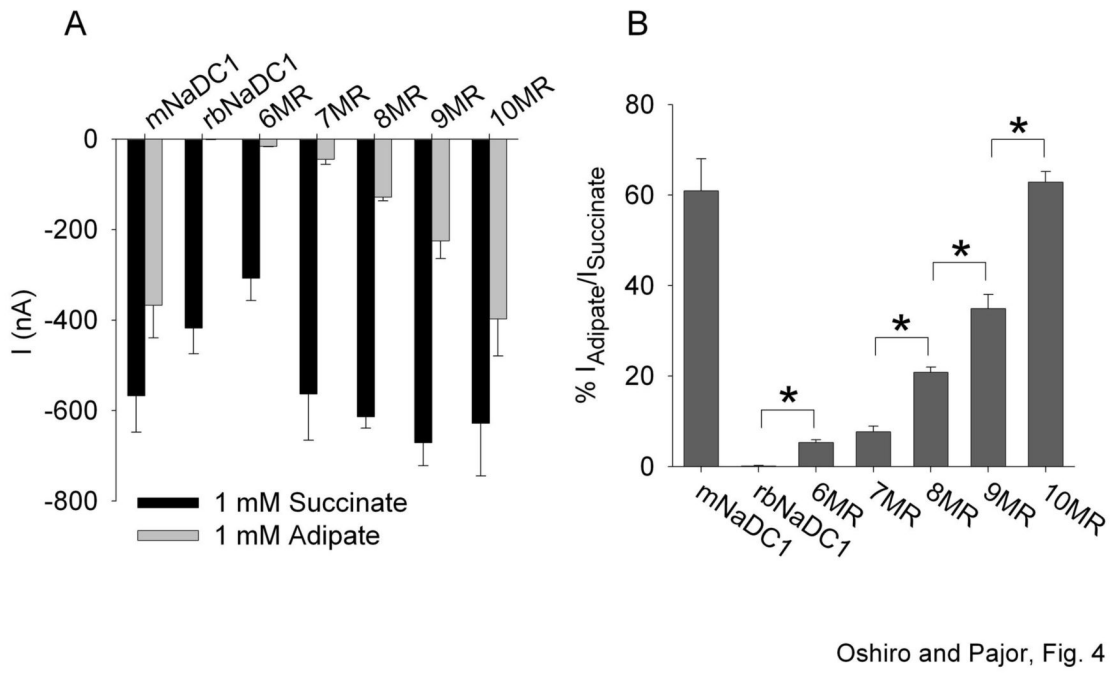

Fig. 4.

Substrate-induced currents mediated by chimeric NaDC1 transporters. (A) Substrate-dependent currents at -50 mV in the presence of 1 mM adipate or succinate in oocytes expressing wild-type and chimeric NaDC1. The bars represent mean ± SEM, n = 14 (mNaDC1), n = 9 (rbNaDC1), n = 3-6 (chimeras). (B) For each oocyte, the adipate-dependent currents were expressed as a percentage of the succinate-dependent currents (data from A). Asterisks represent significant differences, $p < 0.05$.

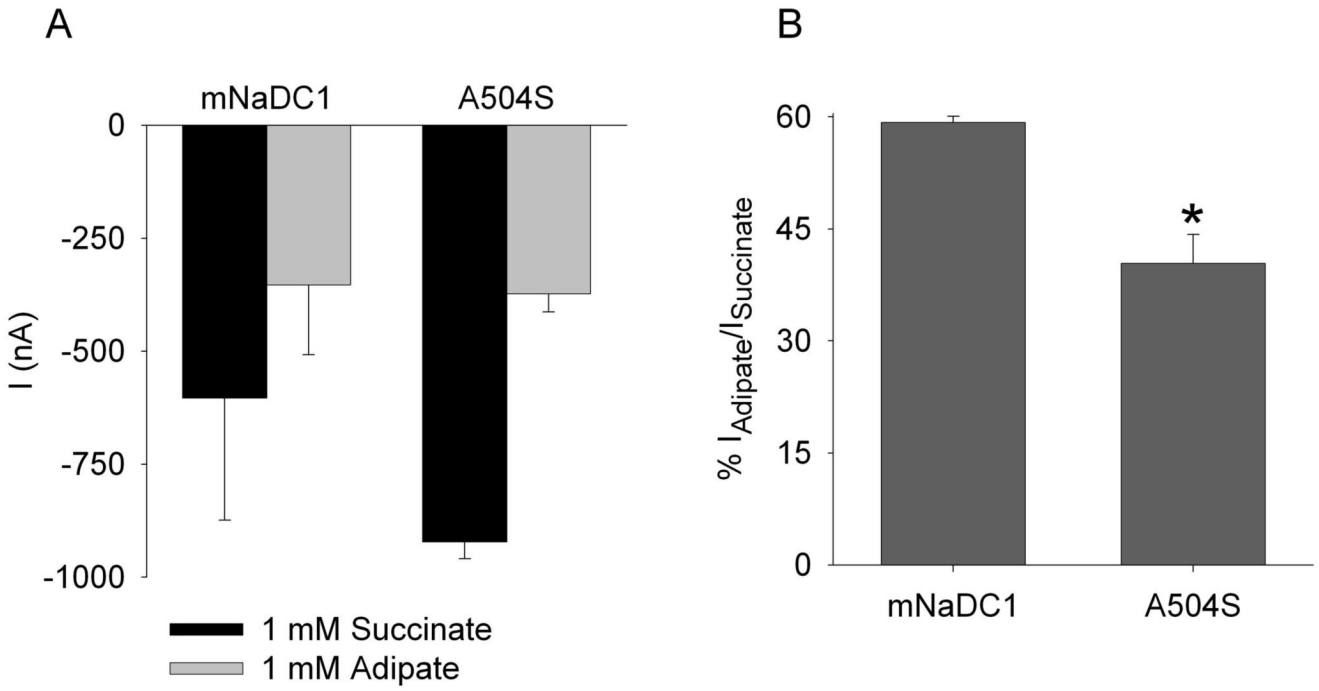

Fig. 5.

Substrate-dependent currents in the A504S mutant of mNaDC1. (A) Adipate- and succinate-induced currents measured at -50 mV with substrate concentrations of 1 mM. The bars represent mean ± SEM, n = 3 paired experiments. (B) Adipate-dependent currents expressed as a percentage of the succinate-dependent currents (from A). The A504S mutant is significantly different from the parental mNaDC1 transporter, $p < 0.05$.

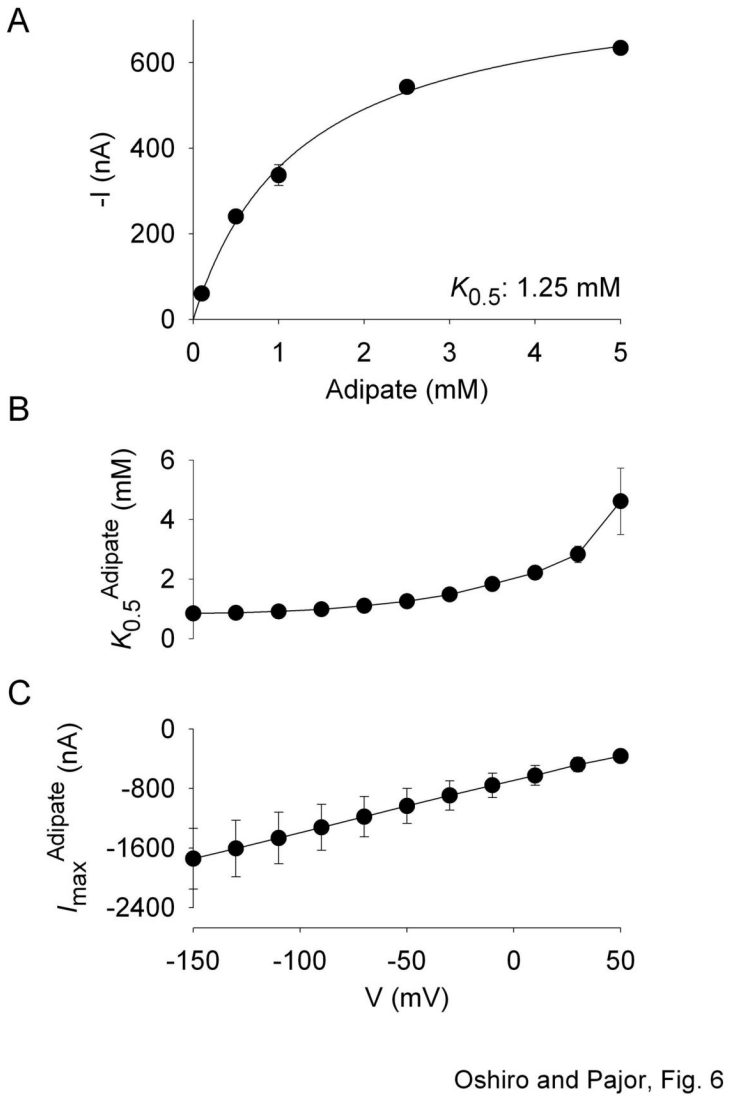

Fig. 6.

Adipate kinetics in oocytes expressing the mNaDC1-A504S mutant. (A) The concentration dependence of the steady-state adipate-induced currents at -50 mV in a single oocyte expressing the A504S mutant. Each data point represents mean ± range of duplicatemeasurements in a single oocyte. The adipate concentrations were between 0.01 mM and 2.5 mM. The $K_{0.5}$ for adipate is 1.25 mM and I_{max} is -797 nA. The voltage dependence of the (B) $K_{0.5}$ and (C) I_{max} for adipate. The data shown are mean ± SEM, n = 3 frogs.

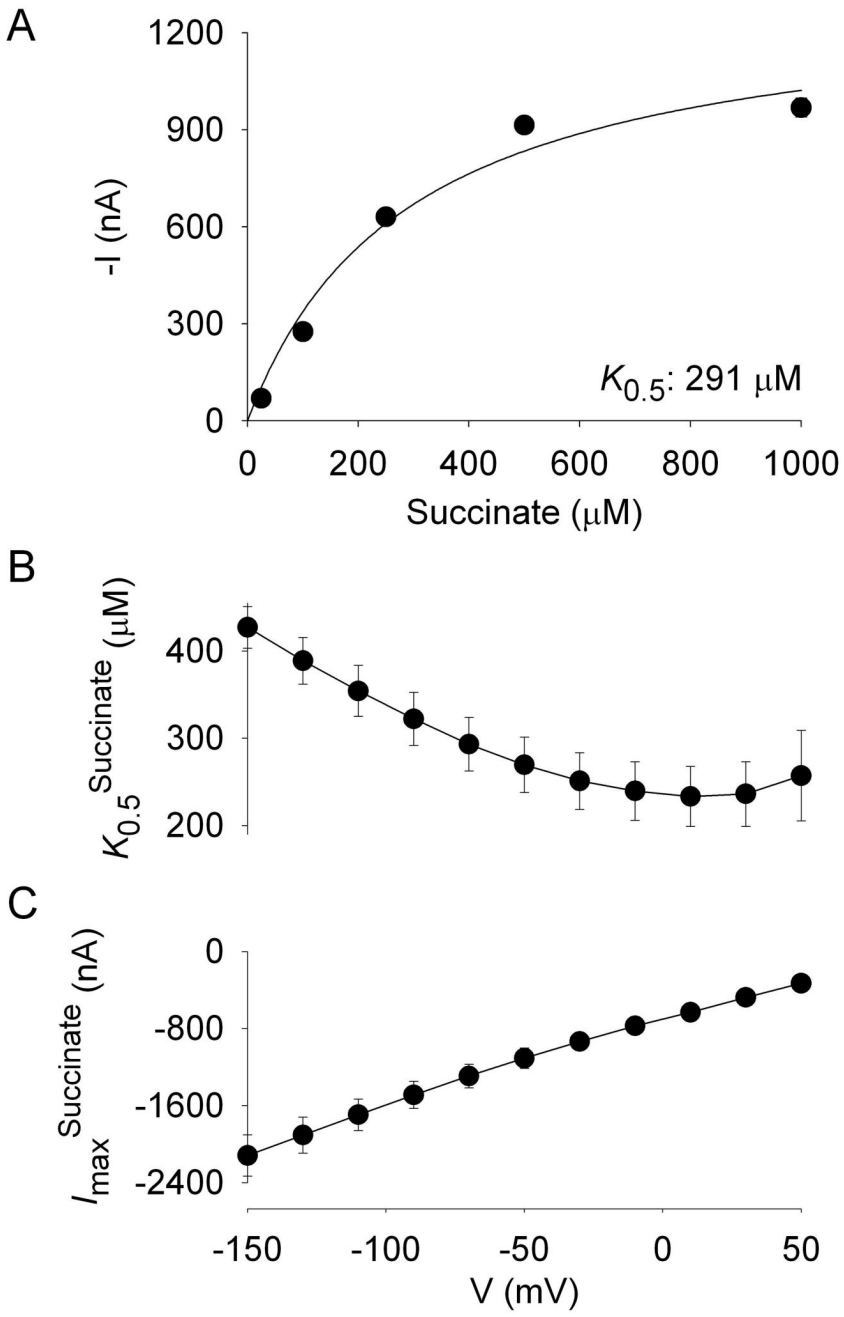

Fig. 7.

Succinate kinetics in the mNaDC1-A504S mutant. (A) Steady-state succinate-induced currents at -50 mV in the presence of different concentrations of succinate between 25 μM and 1 mM. Duplicate measurements in a single oocyte are expressed as mean ± range at each data point. The $K_{0.5}$ for succinate is 291 μM and I_{max} is -1319 nA. The (B) $K_{0.5}$ and (C) I_{max} for succinate at different voltages. The data shown are mean ± SEM, n = 3 frogs.